Kaon B parameter with Wilson fermions

Rajan Gupta and David Daniel
Los Alamos National Laboratory, T-8, MS-B285, Los Alamos, New Mexico 87545

Gregory W. Kilcup
Physics Department, Ohio State University, Columbus, Ohio 43210

Apoorva Patel
Supercomputer Education and Research Centre and Centre for Theoretical Studies, Indian Institute of Science, Bangalore 560012, India

Stephen R. Sharpe
Physics Department FM-15, University of Washington, Seattle, Washington 98195
(Received 9 November 1992)

We calculate the kaon B parameter in quenched lattice QCD at $\beta=6.0$ using Wilson fermions at $\kappa=0.154$ and 0.155. We use two kinds of nonlocal ("smeared") sources for quark propagators to calculate the matrix elements between states of definite momentum. The use of smeared sources yields results with much smaller errors than obtained in previous calculations with Wilson fermions. By combining results for $\mathbf{p}=(0,0,0)$ and $\mathbf{p}=(0,0,1)$, we show that one can carry out the noperturbative subtraction necessary to remove the dominant lattice artifacts induced by the chiral-symmetry-breaking term in the Wilson action. Our final results are in good agreement with those obtained using staggered fermions. We also present results for B parameters of the $\Delta I=\frac{3}{2}$ part of the electromagnetic penguin operators, and preliminary results for B_K in the presence of two flavors of dynamical quarks.

PACS number(s): 12.38.Gc, 11.15.Ha, 14.40.Aq

I. INTRODUCTION

Present calculations of weak matrix elements in the quenched approximation with Wilson fermions suffer from two main sources of error: (i) the signal is poor and (ii) there are large $O(a)$ corrections due to lack of chiral symmetry [1,2]. In this paper we investigate the calculation of the matrix elements of four-fermion operators between pseudoscalar states, and in particular B_K. To improve the signal we calculate the three-point function by sandwiching the operator between kaons produced by smeared sources. This trick has been used to obtain very accurate results with staggered fermions [3]. In order to reduce the $O(a)$ artifacts we use a momentum-subtraction technique that has been tried earlier by the ELC Collaboration [4]. We find that the combined method reduces the statistical errors for all four-fermion operators we have looked at, and allows us to perform nonperturbative subtractions for removing two of the three-chiral-symmetry-violating terms in B_K.

The $O(a)$ corrections arise due to mixing between operators of different tensor structure induced by the explicit chiral-symmetry-breaking term introduced by Wilson to remove lattice doublers. In principle this mixing can be calculated in perturbation theory, but there are large nonperturbative effects at values of g used in lattice calculations. There are two approaches to improving the situation: one is to work with an improved action so that the mixing occurs at $O(g^2a)$ and $O(a^2)$ rather than at $O(a)$ [5], and the second is to devise nonperturbative methods to subtract off the lattice artifacts. It is likely that the eventual solution will be a combination of the two methods. To this end we demonstrate that the calculation of matrix elements within states of definite lattice momentum works for $\mathbf{p}=(0,0,0)$ and (0,0,1), and furthermore that one can reliably carry out a nonperturbative subtraction using these two values of momentum. We use the kaon B parameter as the testing ground for two reasons: (a) there are very accurate results available using staggered fermions on the same set of lattices against which we may compare our results, and (b) there is no mixing with operators of lower dimension.

To make our nonperturbative method work we need two kinds of hadron source: one that produces hadrons with zero momentum and the other that couples to all momenta. We construct zero-momentum hadron correlators using wall source quark propagators, while the Wuppertal source [6] propagators yield hadron correlators that have overlap with all momenta. We have shown in Ref. [7] that these two kinds of correlators yield reliable signals for both the amplitude and the mass extracted from two-point correlation functions. That paper describes in detail the lattices used in the calculation and details of the quark propagators and hadron correlators. It also contains results for hadron masses and decay constants obtained from two-point correlation functions. We use 35 lattices of size $16^3\times 40$ at $\beta\equiv 6g^{-2}=6.0$ with quark propagators calculated at $\kappa=0.154$ and 0.155. The two values of κ correspond to kaons of mass $M_K=700$ and 560 MeV, respectively, using $a^{-1}=1.9$ GeV.

The most accurate results for B_K at $\beta=6.0$ have been obtained with staggered fermions [3]:

$$B_K=\begin{cases}0.70\pm0.02 & (16^3\times40 \text{ lattices}),\\ 0.70\pm0.01 & (24^3\times40 \text{ lattices}).\end{cases} \tag{1.1}$$

There are two previous estimates of B_K with Wilson fermions at $\beta=6.0$. The results of Bernard and Soni are [2]

$$B_K=\begin{cases}0.83\pm0.11\pm0.11 & (16^3\times40 \text{ lattices}),\\ 0.66\pm0.08\pm0.04 & (24^3\times40 \text{ lattices}),\end{cases} \tag{1.2}$$

and those of the ELC Collaboration are (we quote their results obtained on $10^2\times20\times40$ lattices using a linear as well as a quadratic extrapolation) [1]

$$B_K=\begin{cases}0.81\pm0.16 & (\text{linear}),\\ 0.75\pm0.20 & (\text{quadratic}).\end{cases} \tag{1.3}$$

In all calculations the lattice kaon consisted of two almost degenerate quarks (the ratio $m_s/m_u\leq3$). The above results were obtained after interpolation and/or extrapolation of the lattice data to a kaon mass of 495 MeV. The large spread in these numbers and the systematic errors due to bad chiral behavior induced by the Wilson term underscore the need for further improvements and new methods.

We also calculate the B parameter for the $\Delta I=\frac{3}{2}$ part of the electromagnetic penguin operators $\mathcal{O}_7$ and $\mathcal{O}_8$. Previous calculations with both Wilson [8,9] and staggered fermions [10] show that reliable results for the matrix elements of these LR operators can be obtained in lattice calculations and that the vacuum saturation approximation (VSA) provides a good estimate, i.e., $B_{7,8}^{3/2}=1.0\pm0.1$. Our estimates are 0.89(4) and 0.93(5), respectively, and we find that the dominant contribution to the matrix elements of both the LR operators and their VSA comes from the pseudoscalar $\otimes$ pseudoscalar ($\mathcal{P}$) part of the four-fermion operator. Our data show that matrix elements of $\mathcal{P}$ are larger by a factor of 10 or more than other tensor structures and that the two-color loop contraction is roughly 3 times larger than the one-color loop. Furthermore, as the operator $\mathcal{P}$ is not suppressed in the chiral limit, we believe that the VSA will be a good approximation in cases where the operator or its Fierz transform contains $\mathcal{P}$ at the tree level.

This paper is organized as follows. In Sec. II we review the problem induced by the Wilson r term and our partial solution for subtracting lattice artifacts. In Sec. III we describe the lattice methods and in Sec. IV we present our results for B_K. We make a comparison with earlier results obtained with both Wilson and staggered fermions in Sec. V. Section VI presents preliminary results for B_K with two flavors of dynamical quarks. The analysis of the LR operators is given in Sec. VII and we end with conclusions in Sec. VIII.

II. B_K AND THE PROBLEM OF BAD CHIRAL BEHAVIOR

Weak interactions give rise to mixing between the K^0 and the $\overline{K^0}$. The relevant operator in the low-energy effective weak Hamiltonian is the $\Delta S=2$ four-fermion operator $(\bar{s}\gamma_\mu Ld)(\bar{s}\gamma_\mu Ld)$, where we use the notation $L=(1-\gamma_5)$ and $R=(1+\gamma_5)$. The value of the matrix element of this operator between a K^0 and a $\overline{K^0}$ at a typical hadronic scale is severely influenced by strong interaction effects. It has become customary to parametrize this matrix element by the kaon B parameter B_K, which measures the deviation from its value in the VSA:

$$\langle\overline{K^0}|(\bar{s}\gamma_\mu Ld)(\bar{s}\gamma_\mu Ld)|K^0\rangle=\tfrac{8}{3}f_K^2M_K^2B_K\ , \tag{2.1}$$

where parentheses indicate a trace over the spin and color indices. The normalization used for the decay constant is such that $f_\pi=132$ MeV. If the VSA is exact, then $B_K=1$. To calculate B_K from first principles we must turn to nonperturbative methods such as the lattice calculation. Our lattice calculation of B_K uses Wilson's formulation for fermions. The inherent violation of chiral symmetry in this approach leads to technical difficulties which we now review.

To begin with, note that $(\bar{s}\gamma_\mu Ld)(\bar{s}\gamma_\mu Ld)$ is a special case of the operator

$$\mathcal{O}_+=\tfrac{1}{2}[(\bar{\psi}_1\gamma_\mu L\psi_2)(\bar{\psi}_3\gamma_\mu L\psi_4)+(2\leftrightarrow4)]\ , \tag{2.2}$$

with $\psi_1=\psi_3=s$ and $\psi_2=\psi_4=d$. The significance of this is that with a chirally invariant regulator $\mathcal{O}_+$ is multiplicatively renormalized. With Wilson fermions, however, this is not the case: there is mixing of this LL operator with other tensor structures in addition to an overall renormalization, and this complicates the definition of a lattice operator with the desired continuum behavior. In perturbation theory, the corrected operator has been calculated to one-loop in Refs. [11] and [12]:

$$\begin{aligned}\mathcal{O}_+^{\text{cont}}=&\left[1+\frac{g^2}{16\pi^2}Z_+(r,a\mu)\right]\mathcal{O}_+^{\text{latt}}\\&+\frac{4g^2}{16\pi^2}r^2Z^*(r)(\mathcal{O}_+^{STP}+\mathcal{O}_+^{VA}+\mathcal{O}_+^{SP})\ ,\end{aligned} \tag{2.3}$$

where

$$\begin{aligned}\mathcal{O}_+^{STP}&=\frac{N-1}{16N}[(\mathcal{S}+\mathcal{T}+\mathcal{P})+(2\leftrightarrow4)]\ ,\\ \mathcal{O}_+^{VA}&=-\frac{N^2+N-1}{32N}[(\mathcal{V}-\mathcal{A})+(2\leftrightarrow4)]\ ,\\ \mathcal{O}_+^{SP}&=-\frac{1}{16N}[(\mathcal{S}-\mathcal{P})+(2\leftrightarrow4)]\ ,\end{aligned} \tag{2.4}$$

and $N=3$ is the number of colors. We have used a condensed notation for the allowed Lorentz tensor structures:

$$\begin{aligned}\mathcal{S}&=(\bar{\psi}_1\psi_2)(\bar{\psi}_3\psi_4)\ ,\\ \mathcal{V}&=(\bar{\psi}_1\gamma_\mu\psi_2)(\bar{\psi}_3\psi_\mu\psi_4)\ ,\\ \mathcal{T}&=\sum_{\mu<\nu}(\bar{\psi}_1\sigma_{\mu\nu}\psi_2)(\bar{\psi}_3\sigma_{\mu\nu}\psi_4)\ ,\\ \mathcal{A}&=(\bar{\psi}_1\gamma_\mu\gamma_5\psi_2)(\bar{\psi}_3\gamma_\mu\gamma_5\psi_4)\ ,\\ \mathcal{P}&=(\bar{\psi}_1\gamma_5\psi_2)(\bar{\psi}_3\gamma_5\psi_4)\ ,\end{aligned} \tag{2.5}$$

where γ_μ, γ_5 are Hermitian and $\sigma_{\mu\nu}=(\gamma_\mu\gamma_\nu-\gamma_\nu\gamma_\mu)/2$. We note that the Fierz transform eigenstates appearing in Eq. (2.3) are only $(\mathcal{V}+\mathcal{A})$, $\frac{1}{2}(\mathcal{V}-\mathcal{A})\pm(\mathcal{S}-\mathcal{P})$, and $(\mathcal{S}+\mathcal{T}+\mathcal{P})$; there is also no mixing between the fifth eigenstate of the Fierz transformation $(\mathcal{S}-\frac{1}{3}\mathcal{T}+\mathcal{P})$ and the operator $\mathcal{O}_+$ and one-loop. There is no mixing with lower-dimensional operators, for the simple reason that there are *no* $\Delta S=2$ operators of lower dimension. We shall henceforth denote the perturbatively corrected $(\bar{s}\gamma_\mu Ld)(\bar{s}\gamma_\mu Ld)$ operator [cf. Eq. (2.3)] by $\hat{\mathcal{O}}$.

The renormalization coefficients for Wilson parameter $r=1$ are given in Table I in three schemes: the dimensional reduction (DRED) used by Altarelli *et al.* [13] and Martinelli [11], as well as the "naive" dimensional regularization (NDR) and the dimensional reduction with an easy subtraction [DR($\overline{\text{EZ}}$)] scheme used by Bernard, Draper, and Soni in [12]. A detailed description of DRED and NDR schemes and their relative advantages and disadvantages is given in Ref. [14]. We tabulate the relevant results in order to provide an easy reference, and to allow the reader to make a rough estimate of the magnitude of the scheme dependence. All our results are given in the DRED scheme, except when we compare raw lattice numbers against those in Ref. [15], in which case we use DR($\overline{\text{EZ}}$).

For each of the four-fermion operators $\mathcal{S}$, $\mathcal{V}$, $\mathcal{T}$, $\mathcal{A}$, and $\mathcal{P}$, there are two distinct contractions with the external states. In the first each bilinear is contracted with an incoming or outgoing kaon corresponding to two spin and two-color traces. We label these contractions by $\mathcal{P}^2$, $\mathcal{S}^2$, $\mathcal{V}^2$, $\mathcal{A}^2$, and $\mathcal{T}^2$. The other contraction consists of a single spin and color trace which we Fierz transform to two spinor loops. We label them by $\mathcal{P}^1$, $\mathcal{S}^1$, $\mathcal{V}^1$, $\mathcal{A}^1$, and $\mathcal{T}^1$, since they have a single color trace. We will find it useful to further split the $\mathcal{V}$, $\mathcal{A}$, and $\mathcal{T}$ terms into their space and time components, and denote these components by subscripts s and t, respectively. This notation is similar to that used with staggered fermions [3] and will facilitate later comparison of results for individual operators between the two formulations.

TABLE I. Summary of one-loop perturbative results for the various Z factors needed in our calculations in three different continuum regularization schemes. The two constants are $C_F=\frac{4}{3}$ and $\lambda=g^2/16\pi^2$. The results in DRED and NDR schemes are the sum of those in DR($\overline{\text{EZ}}$) and the entries in their respective columns. These expressions are extracted from Refs. [11], [12], and [7]. The numerical results are taken from Ref. [12]. In the text all results are given in the DRED scheme used in Ref. [11], except when we compare raw lattice numbers against those in Ref. [15].

	DR($\overline{\text{EZ}}$)	DRED	NDR
Z_A	$1-15.796C_F\lambda$	$0.5C_F\lambda$	0
Z_P	$1+C_F\lambda(6\ln(\mu a)-21.596)$	0	$-C_F\lambda$
Z_+	$-50.174-4\ln(\mu a)$	$\frac{7}{3}$	$\frac{14}{3}$
Z_-	$-45.308+8\ln(\mu a)$	$-\frac{2}{3}$	$-\frac{4}{3}$
Z_1	$-49.364-2\ln(\mu a)$	$\frac{11}{6}$	$\frac{11}{3}$
Z_2	$-42.064+16\ln(\mu a)$	$-\frac{8}{3}$	$-\frac{16}{3}$
Z^*	9.6431	0	0

In order to extract B_K, we calculate, at nonzero-momentum transfer, the matrix element

$$\mathcal{M}_K(\mathbf{p})=\langle\overline{K^0}(\mathbf{p})|\hat{\mathcal{O}}(\mathbf{p})|K^0(\mathbf{p}=0)\rangle\ . \tag{2.6}$$

In chiral perturbation theory $\mathcal{M}_K(\mathbf{p})$ behaves as $\sim\gamma_K p_K\cdot p_{\bar{K}}$, where $\gamma_K=8/3f_K^2B_K$, and p_K and $p_{\bar{K}}$ are the on-shell four-momenta of the external states, so that $p_K\cdot p_{\bar{K}}=M_K\sqrt{M_K^2+(\mathbf{p})^2}$. Unfortunately, on the lattice with Wilson fermions chiral symmetry is explicitly broken and the expansion becomes

$$\mathcal{M}_K(\mathbf{p})=\alpha+\beta M_K^2+(\gamma+\gamma_K)p_K\cdot p_{\bar{K}}+\cdots\ , \tag{2.7}$$

where the ellipsis represents terms of higher order in p^2 or M_K^2. The terms proportional to α, β, and γ are unphysical contributions arising from the r term in the Wilson action. The same formula also holds for off-shell matrix elements (i.e., $\langle 0|\hat{\mathcal{O}}|K^0K^0\rangle$).

Using the perturbatively improved operator $\hat{\mathcal{O}}$ reduces the size of the lattice artifacts, but does not eliminate them completely because it is only an approximation to the desired continuum operator. In particular, there is mixing with operators having the wrong chiral behavior at $O(rg^4)$. As we discuss below, this apparently tiny effect can in fact be important. In addition, there are $O(a)$ corrections, which previous calculations have shown to be significant, and which cannot be removed by a perturbative correction to the operator. To isolate the physical coefficient γ_K we therefore require a nonperturbative method.

As discussed below, we expect the most troublesome of the lattice artifacts to be α. Failure to correctly subtract this contamination will mean that B_K will diverge in the chiral limit. To eliminate this, it is not necessary to work at nonzero-momentum transfer. One can simply calculate $\mathcal{M}_K(\mathbf{p}=0)$ at different values of κ (that is, different values of M_K) and take a difference, leaving

$$\mathcal{M}_K(\kappa,\mathbf{p}=0)-\mathcal{M}_K(\tilde{\kappa},\mathbf{p}=0)=(\beta+\gamma+\gamma_K)(M_K^2-\tilde{M}_K^2)\ . \tag{2.8}$$

To remove β one takes the difference of the on-shell and off-shell matrix elements. This method has been used in Refs. [1] and [2], and suffers from the lack of control over final-state interactions between the kaons in the off-shell amplitude. A review of the status of previous results is given in Refs. [16] and [17].

We advocate instead using momentum subtraction with only on-shell matrix elements, which eliminates both α and β at each value of M_K. By calculating the matrix element of $\hat{\mathcal{O}}$ for two values of $\mathbf{p}$ and taking the difference one gets

$$\mathcal{M}_K(\mathbf{p})-\mathcal{M}_K(0)=(\gamma+\gamma_K)M_K(E(p)-M_K)+\cdots\ . \tag{2.9}$$

In fact, this cancels all higher-order terms in the chiral expansion dependent on M_K^2 alone. In practice we calculate

$$B_K=\frac{E(p)B_K^L(p)-M_KB_K^L(0)}{E(p)-M_K}=\frac{(\gamma+\gamma_K)}{\frac{8}{3}f_K^2}+\cdots \tag{2.10}$$

at each value of κ, where by $B_K^L(p)$ we mean the ratio of the matrix element to its VSA value, both calculated on the lattice at approximate momentum transfer.

There are two shortcomings to this subtraction scheme. The first is that it does not eliminate the lattice artifact γ. It is therefore important to estimate the size of γ relative to γ_K. To do this we assume that lattice artifacts can be represented by mixing with local operators, and that the size of this mixing can be estimated using perturbation theory. This ignores $O(a)$ effects, but the resulting estimate turns out to have the correct order of magnitude. Based on the correction to the operators through $O(g^2)$ [Eq. (2.3)], we estimate the size of the remaining lattice artifacts in $\hat{O}$ to be

$$\delta\mathcal{O}=r\left[10\frac{g^2}{16\pi^2}\right]^2(c_P\mathcal{P}+c_T\mathcal{T}+\cdots),$$

where c_P and c_T are of order 1. Here we have assumed that the typical perturbative coefficient is 10 [as is true for the largest coefficients in Eqs. (2.3) and (4.1)]. If we take $g^2=1.75$ (a reasonable value as discussed below), set $r=1$, and assume $c_P=c_T=1$, the factor multiplying the operators is $\frac{1}{80}$. It is certainly possible that the actual coefficient is somewhat larger (or smaller), but it is clear that the suppression factor is large. In order to overcome this factor, we need only consider operators with large matrix elements. To get a rough estimate, we consider only $\mathcal{P}^2$ (defined below), since this has the largest matrix elements, and assume that it is sufficient to work with the bare lattice operator, i.e., without perturbative corrections. In other words, we assume that

$$\alpha+(\beta+\gamma)M_K^2\approx\langle\bar{K}_0|\delta\mathcal{O}|K_0\rangle\approx\tfrac{1}{80}\langle\bar{K}_0|\mathcal{P}^2|K_0\rangle\ .$$

Converting the results for $B_{\mathcal{P}^2}$ given in Tables II(b) and III(b) to those for matrix elements, and using our final result for B_K, gives the estimates

$$\alpha+(\beta+\gamma)M_K^2=\tfrac{1}{80}[267,254]\times10^{-4}$$
$$=\tfrac{1}{80}[14,25](\gamma+\gamma_K)M_K^2\ .$$

TABLE II. (a) The one-color loop contribution to the lattice B parameters for individual operators at $\kappa=0.154$. Each box shows the χ^2 for a correlated fit, the temporal range of the fit and the fitted value. The space and time components of the operators have been shown separately. The appropriate ratios of correlators have been calculated using two different kaon operators γ_5 and A_4 and using Wuppertal and wall sources. The notation, for example, is as follows: $PS[1]WP$ stands for the four-fermion operator with one unit of lattice momentum sandwiched between Wuppertal and wall source kaons each created with operator γ_5. All errors are calculated using the single elimination jackknife method. (b) The same as (a), but for the two-color loop contribution.

	$PS[0]SP$	$PW[0]WP$	$PS[0]WP$	$PS[1]WP$	$AS[0]SA$	$AW[0]WA$	$AS[0]WA$	$AS[1]WA$
				(a)				
	1.6	1.1	0.3	0.8	1.4	1.2	0.6	0.5
	14–26	14–26	14–26	23–31	12–28	14–26	10–30	22–31
$\mathcal{P}^1$	−4.30(21)	−4.03(17)	−3.99(19)	−2.58(28)	−3.86(35)	−3.86(21)	−3.70(20)	−2.45(27)
	2.3	4.7	2.0	2.0	7.7	4.0	2.8	1.8
	10–30	12–28	12–28	24–33	10–30	11–29	10–30	22–31
$\mathcal{S}^1$	−0.45(4)	−0.42(6)	−0.42(3)	−0.26(5)	−0.38(8)	−0.40(6)	−0.38(4)	−0.26(5)
	2.2	6.0	4.3	1.2	4.0	6.1	3.2	1.8
	16–28	12–28	13–27	26–33	10–30	10–30	10–30	22–32
$\mathcal{V}_s^1$	0.40(18)	0.35(10)	0.35(8)	0.10(11)	0.36(9)	0.39(11)	0.31(6)	0.10(10)
	4.3	1.3	1.1	0.8	2.3	1.2	2.7	0.9
	11–29	12–28	14–26	26–33	15–25	14–26	10–30	22–31
$\mathcal{V}_t^1$	0.24(6)	0.22(2)	0.21(2)	0.12(2)	0.22(3)	0.20(2)	0.22(2)	0.11(3)
	3.5	2.0	2.2	0.2	2.2	2.7	2.0	0.4
	12–28	12–28	11–29	25–34	10–30	14–26	10–30	26–33
$\mathcal{A}_s^1$	−0.60(6)	−0.56(6)	−0.56(5)	−0.33(4)	−0.54(3)	−0.50(5)	−0.52(6)	−0.28(6)
	3.8	1.0	4.2	2.9	0.8	1.4	0.6	1.6
	12–28	14–26	9–31	27–33	14–26	14–26	14–26	27–35
$\mathcal{A}_t^1$	0.11(2)	0.12(2)	0.10(2)	0.15(3)	0.10(3)	0.12(2)	0.09(1)	0.15(4)
	1.8	1.5	0.9	1.9	0.6	2.8	1.1	0.7
	10–30	15–25	10–30	25–34	16–24	12–28	10–30	23–31
$\mathcal{T}_s^1$	2.84(21)	2.63(10)	2.70(10)	1.59(18)	2.56(34)	2.59(14)	2.51(16)	1.54(16)
	3.3	1.0	0.7	1.1	1.5	2.5	0.6	1.2
	14–26	15–25	10–30	25–32	12–24	14–26	12–28	24–31
$\mathcal{T}_t^1$	2.93(24)	2.73(10)	2.79(12)	1.70(21)	2.67(36)	2.66(17)	2.58(17)	1.66(20)

TABLE II. (*Continued*).

	$PS[0]SP$	$PW[0]WP$	$PS[0]WP$	$PS[1]WP$	$AS[0]SA$	$AW[0]WA$	$AS[0]WA$	$AS[1]WA$
				(b)				
	1.6	0.9	0.4	0.8	1.6	1.1	0.8	0.6
	12–28	12–28	10–30	23–32	12–28	14–26	9–31	22–31
$\mathcal{P}^2$	−12.09(75)	−11.60(50)	−11.26(43)	−7.15(75)	−10.99(95)	−11.05(60)	−10.77(54)	−6.81(68)
	2.9	2.7	2.8	1.7	2.7	1.3	2.0	1.8
	10–30	14–26	14–26	25–33	12–28	14–26	10–30	22–31
$\mathcal{S}^2$	−0.60(10)	−0.51(9)	−0.49(6)	−0.40(8)	−0.47(14)	−0.49(6)	−0.52(7)	−0.38(7)
	1.2	1.3	1.1	0.6	3.0	2.5	1.6	1.6
	15–25	14–26	12–28	25–34	10–30	14–32	10–32	26–33
$\mathcal{V}_s^2$	0.03(3)	0.04(2)	0.05(2)	0.01(2)	0.04(3)	0.04(3)	0.04(2)	−0.02(3)
	1.0	2.1	1.8	1.3	2.8	2.1	2.2	1.5
	14–26	14–26	10–30	25–34	12–28	14–26	10–30	24–31
$\mathcal{V}_t^2$	0.02(0)	0.02(1)	0.02(0)	0.01(1)	0.02(0)	0.02(1)	0.02(0)	0.02(1)
	5.1	2.4	1.9	2.1	2.4	2.1	1.9	1.2
	8–32	11–26	10–30	25–34	10–30	14–26	10–30	25–33
$\mathcal{A}_s^2$	−0.54(5)	−0.52(4)	−0.53(4)	−0.31(3)	−0.50(7)	−0.49(4)	−0.49(5)	−0.25(4)
	3.4	4.2	1.3	0.8	2.8	3.3	0.7	0.8
	13–24	10–25	15–25	25–33	12–24	14–26	16–24	24–32
$\mathcal{A}_t^2$	0.64(4)	0.62(3)	0.58(2)	0.64(8)	0.56(5)	0.58(7)	0.54(3)	0.60(7)
	5.3	3.6	3.2	2.0	3.6	3.9	3.0	1.5
	10–30	12–28	10–30	28–34	12–28	14–26	10–30	23–35
$\mathcal{T}_s^2$	0.05(2)	0.06(2)	0.05(1)	0.03(1)	0.05(2)	0.05(1)	0.04(2)	0.04(1)
	7.1	1.5	2.3	1.0	3.7	2.1	4.1	1.1
	14–26	14–26	10–30	25–33	8–31	14–26	6–34	26–33
$\mathcal{T}_t^2$	0.07(2)	0.05(1)	0.05(1)	0.03(1)	0.03(5)	0.04(3)	0.06(2)	0.05(1)

The two results are for $\kappa=[0.154,0.155]$. This shows that the matrix elements provide fairly large enhancement factors, which, if there are no cancellations between operators in $\delta\mathcal{O}$, can overcome the factor $\frac{1}{80}$. This estimate suggests that the lattice artifacts can be 20%–30% of the signal. In fact, we find in Sec. IV that the artifact is 2–3 times larger than this. Given the crudeness of this estimate, however, we consider the agreement reasonable. We mention in passing that Bernard and Soni have advocated a scheme based on such an analysis to subtract the unphysical terms [2].

The second part of our estimate is of the ratio $\gamma M_K^2/(\alpha+\beta M_K^2)$ for our values of the kaon mass. We calculate $\alpha,\beta M_K^2$, and γM_K^2 for the two dominant operators $\mathcal{P}$ and $\mathcal{T}$ using the results in Tables II and III. Neglecting perturbative corrections to the operators, we find that $\mathcal{P}^1$, $\mathcal{P}^2$, and $\mathcal{T}^1$ all give similar results:

$$\frac{\gamma M_K^2}{\alpha+\beta M_K^2}\approx -0.3(0.3), \quad \frac{\beta M_K^2}{\alpha}\approx 0.3\ ,$$

at the two kaon masses. This is the basis for our assertion that α is the dominant lattice artifact. It also shows that, if the entire lattice artifact is of the same size as the signal, as we find to be roughly true, then $|\gamma/\gamma_K|\approx 0.3$, a substantial but not overwhelming correction.

Finally, we comment on the second shortcoming of the subtraction method, its reliance on a truncated chiral expansion. The chiral expansion parameter is $p^2/(2\pi f_\pi)^2$. Using $p^2=M_K^2$, this is $\frac{1}{4}$–$\frac{1}{2}$ for our masses. However, it is even larger for our matrix elements at nonzero-momentum transfer, approaching unity. As mentioned above, our subtraction method does not remove corrections of the form $M_K^2 p_K\cdot p_{\bar K}$ or $(p_K\cdot p_{\bar K})^2$. In Sec. IV we make a rough estimate of these terms by comparing the results for B_K from Eq. (2.10) coming from different kaon masses. The corrections are significant, but we are not able to separate the physical contributions from the artifacts. Therefore, the method needs to be tested further on larger lattices so that the minimum nonzero momentum is reduced, and data at a few different momentum transfers can be obtained.

III. METHODOLOGY

Our method for calculating B_K requires that we double the $16^3\times 40$ lattices in the time direction, so that they are of size $16^3\times 80$. On these doubled lattices we construct hadron correctors such that the correlator on time slices

TABLE III. (a) The same as in Table II(a) but for $\kappa=0.155$. (b) The same as (a), but for the two-color loop contribution.

	$PS[0]SP$	$PW[0]WP$	$PS[0]WP$	$PS[1]WP$	$AS[0]SA$	$AW[0]WA$	$AS[0]WA$	$AS[1]WA$
				(a)				
	2.6	0.6	0.5	2.1	1.9	1.8	0.9	0.8
	10–30	16–27	10–30	23–33	12–28	14–28	12–30	26–33
$\mathcal{P}^1$	−7.08(97)	−6.48(41)	−6.49(39)	−3.42(57)	−5.98(71)	−5.99(44)	−5.58(42)	−3.24(42)
	3.2	4.4	1.8	1.4	4.5	3.4	1.5	2.3
	10–30	14–27	11–29	28–33	10–30	14–28	12–30	26–33
$\mathcal{S}^1$	−1.01(18)	−0.92(19)	−0.94(10)	−0.48(13)	−0.85(14)	−0.89(19)	−0.85(10)	−0.48(11)
	5.9	8.7	3.1	1.2	4.6	10.6	3.3	1.1
	13–29	13–27	13–27	25–33	14–32	10–30	12–30	27–34
$\mathcal{V}_s^1$	0.83(65)	0.87(41)	0.91(17)	0.32(18)	0.83(18)	0.83(31)	0.79(18)	0.36(27)
	6.0	2.9	1.5	1.1	5.3	1.5	1.0	0.5
	15–26	11–29	14–26	26–33	11–30	14–28	13–29	26–33
$\mathcal{V}_t^1$	0.38(15)	0.45(9)	0.42(5)	0.22(6)	0.42(9)	0.41(8)	0.40(5)	0.23(7)
	4.4	2.6	1.6	0.3	0.7	3.9	2.2	0.8
	10–30	12–28	14–27	27–33	8–32	12–28	10–30	26–33
$\mathcal{A}_s^1$	−1.02(17)	−1.09(20)	−1.01(12)	−0.49(15)	−0.92(12)	−0.97(19)	−0.89(10)	−0.38(14)
	0.3	4.3	2.9	3.0	1.7	4.2	1.8	2.1
	12–28	10–30	12–28	28–33	10–28	13–27	14–27	25–34
$\mathcal{A}_t^1$	0.01(5)	−0.01(3)	−0.03(3)	0.12(7)	−0.01(4)	0.02(5)	−0.01(3)	0.14(9)
	3.9	4.9	0.9	1.8	1.2	4.0	1.1	0.9
	12–28	12–30	11–29	26–33	12–24	14–28	11–29	26–33
$\mathcal{T}_s^1$	5.66(69)	5.09(59)	5.27(30)	2.73(52)	4.90(91)	4.79(66)	4.75(39)	2.76(47)
	4.0	2.9	0.7	2.3	2.5	3.1	1.3	1.5
	12–28	13–30	12–28	26–33	13–25	14–28	10–30	26–33
$\mathcal{T}_t^1$	5.86(77)	5.39(49)	5.38(32)	3.24(48)	4.87(121)	5.01(46)	4.93(30)	2.96(48)
				(b)				
	2.6	2.7	0.6	1.0	2.0	1.6	0.9	0.8
	10–30	13–29	10–30	24–32	12–28	14–28	11–29	26–33
$\mathcal{P}^2$	−19.7(26)	−18.4(15)	−18.0(11)	−9.0(15)	−16.7(23)	−16.8(13)	−15.8(12)	−9.0(11)
	2.7	4.0	2.4	1.3	2.2	3.3	1.1	2.2
	10–30	13–27	10–30	26–35	12–28	14–28	15–27	26–33
$\mathcal{S}^2$	−1.45(32)	−1.44(33)	−1.43(17)	−0.94(23)	−0.98(31)	−1.24(14)	−1.05(24)	−0.82(15)
	5.2	3.9	1.0	1.4	1.6	2.5	1.0	1.6
	11–29	14–28	12–26	26–33	14–27	16–30	12–28	27–32
$\mathcal{V}_s^2$	0.07(4)	0.06(4)	0.08(2)	0.00(4)	0.13(11)	0.02(7)	0.05(4)	−0.08(9)
	3.8	3.4	2.0	1.4	4.6	4.3	1.7	1.3
	12–28	14–27	10–30	26–33	14–27	14–28	15–27	26–31
$\mathcal{V}_t^2$	0.04(1)	0.04(1)	0.04(1)	0.01(1)	0.02(3)	0.04(2)	0.03(1)	0.03(2)
	7.4	3.6	2.5	1.8	2.8	1.5	1.4	1.3
	12–28	11–31	10–30	26–35	14–27	15–27	11–29	26–34
$\mathcal{A}_s^2$	−1.06(17)	−0.96(6)	−0.97(9)	−0.52(9)	−0.89(14)	−0.86(8)	−0.87(13)	−0.42(8)
	0.1	3.9	1.9	1.2	0.3	5.9	1.4	1.1
	12–28	15–25	16–24	26–33	12–28	14–28	12–25	28–34
$\mathcal{A}_t^2$	0.57(10)	0.51(9)	0.49(9)	0.61(13)	0.49(10)	0.48(11)	0.45(4)	0.53(8)
	4.0	3.3	2.6	2.2	4.2	3.8	4.1	2.1
	15–25	13–27	14–27	28–34	12–28	14–28	9–31	26–33
$\mathcal{T}_s^2$	0.14(6)	0.13(3)	0.14(3)	0.03(2)	0.09(3)	0.11(3)	0.11(4)	0.06(3)
	4.4	1.6	2.6	1.0	1.9	3.0	1.8	0.8
	14–27	14–27	12–28	26–33	14–26	17–26	10–30	26–35
$\mathcal{T}_t^2$	0.15(4)	0.14(1)	0.14(2)	0.05(2)	0.06(5)	0.12(8)	0.13(4)	0.07(2)

1–39 is the forward moving particle with the source at time slice 0, while the correlator on time slices 79–41 is the backward moving particle with the periodically reflected source on time slice 80. To calculate matrix elements we insert the operator between these "forward" and "backward" moving particles on the original $16^3\times 40$ lattices.

We use various results from Ref. [7] to interpret our data. For $\kappa=[0.154,0.155]$, we use $M_K=[0.364,0.297]$, $f_K=[0.0815,0.0779]$ and $E_K=[0.51,0.47]$, where the latter quantity is the energy of the kaon with momentum $\mathbf{p}=(1,0,0)$. All results are in lattice units.

In practice, we divide the correlators for the various matrix elements by the product of kaon correlators, so that we directly obtain the B parameters for the various operators $\mathcal{O}$:

$$B_{\mathcal{O}}\equiv\frac{3}{8}\frac{\langle\overline{K^0}(\mathbf{p})|\mathcal{O}|K^0(\mathbf{p}=0)\rangle}{\langle\overline{K^0}(\mathbf{p})|A_4|0\rangle\langle 0|A_4|K^0(\mathbf{p}=0)\rangle}\ . \tag{3.1}$$

We can select the kaon momenta by our choice of source and by inserting momentum into the operator $\mathcal{O}$. The statistical errors are reduced because we can average the operator location over a time slice of the lattice. Away from the sources, only the lightest state contributes to the correlators, and we should find a time-independent plateau giving $B_{\mathcal{O}}$. This method is similar to the one we have used successfully with staggered fermions [3].

The physical picture of the process for calculating matrix elements using smeared sources is as follows: a wall source at $t=0$ produces zero momentum K^0 which propagates for a time t, at which point the operator inserts momentum $\mathbf{p}$, and the resulting $\overline{K^0}$ with momentum $\mathbf{p}$ then propagates the remaining (N_t-t) time slices until it is destroyed by a Wuppertal source. Three factors are essential for our method to work.

(i) The wall source creates only zero-momentum kaons; otherwise there is contamination from matrix elements of kaons with other momenta.

(ii) The Wuppertal source has significant overlap with the lowest few momenta allowed on the lattice.

(iii) For matrix elements involving $\mathbf{p}\neq 0$ kaons, we must ensure that there exists an overlap region for the kaons where a plateau can be observed in the B-parameter signal. Thus it is essential that the signal for the zero-momentum kaon produced by the wall source extends across the lattice to the region where there is a signal for the nonzero-momentum kaon produced by the Wuppertal source.

In Ref. [7] we showed that these conditions are satisfied by the Wuppertal and wall correlators, when we use $\mathbf{p}=(0,0,0)$ and $\mathbf{p}=(0,0,1)$. Furthermore, there are a number of consistency checks we make.

(1) The $\mathbf{p}=0$ matrix element is calculated three different ways: (a) using wall sources on both sides, (b) using a wall source on one side and a Wuppertal source on the other, and (c) using Wuppertal sources on both sides [in this case there is a small contamination from the $\mathbf{p}=(0,0,1)$ state].

(2) We use two kaon source operators: γ_5 and A_4. The plateau in each individual $B_{\mathcal{O}}$ is reached from opposite directions for these two. The two results should converge to the same value.

As shown in Tables II(a)–III(b) these checks are satisfied by our data within the statistical accuracy. We also find that the B parameter for the operators $\mathcal{A}_t^2$ and $\mathcal{P}^2$ are within a factor of 2 of their VSA values. As in the case of staggered fermions, the final value of B_K is obtained after a large cancellation between the $\mathcal{A}$ and $\mathcal{V}$ components showing that the VSA is not a good approximation.

IV. RESULTS FOR B_K

Our final lattice result at a given value of κ and $\mathbf{p}$ is obtained from the perturbatively improved combination (using the convention that all four quarks have distinct flavor labels so that each term has just one Wick contraction)

$$Z_A^2 B_K^L(\mathbf{p})=\left[1+\frac{g^2}{16\pi^2}Z_+(r,a\mu)\right](\mathcal{V}^1+\mathcal{V}^2+\mathcal{A}^1+\mathcal{A}^2)$$
$$+\frac{g^2}{16\pi^2}\frac{r^2Z^*(r)}{12}[(26\mathcal{S}^1+2\mathcal{S}^2)-(18\mathcal{P}^1-6\mathcal{P}^2)+4(\mathcal{T}^1+\mathcal{T}^2)+(\mathcal{V}^1-\mathcal{A}^1)-11(\mathcal{V}^2-\mathcal{A}^2)]\ . \tag{4.1}$$

For simplicity, we have here used the operator symbol to denote its B parameter. The one-loop perturbative results for the renormalization constants Z_A and Z_+ are given in Table I. Note that the finite part of the renormalization factor $(1+(g^2/16\pi^2)Z_+)$ is largely canceled by Z_A^2 for $g^2\lesssim 1$.

We give the results for the individual $B_{\mathcal{O}}$ (without any g^2 corrections) at $\kappa=0.154$ and 0.155 in Tables II(a)–III(b). In all cases we find that the signal in the ratio of correlators is significantly better with the operator γ_5 as the kaon source than with the operator A_4, even though the two sets give consistent results. As an example, we show a comparison of the two signals in Figs. 1(a) and 1(b). Our final results therefore use the γ_5 numbers.

We point out that in case of nonzero-momentum transfer, the signal for $B_{\mathcal{O}}$ only exists closer to the Wuppertal source (at time slice "40") than the wall source (at time slice "0"). This is because the signal in the $\mathbf{p}=(0,0,1)$ kaon correlators only extends for about 20 time slices. The overall quality of the signal for B_K^L (with $g^2=1$, $\mu a=1.0$) is shown in Figs. 1–4 at various values of κ and $\mathbf{p}$.

Tables II(a)–III(b) show that all individual $B_{\mathcal{O}}$, except for $B_{\mathcal{A}_t}$, increase by a factor of about 2 between $\kappa=0.154$ and 0.155. This increase is largely due to the change in the VSA, i.e., the factor $f_K^2M_K^2$ decreases by approximately 1.9 between the two κ values [7]. This shows that

at these values of κ, the lattice matrix elements are dominated by the constant term α.

The contribution of the mixing terms to B_K^L can be large only if the matrix elements are large, since the perturbative mixing coefficient is ≈ 0.005 for $g^2=1$. The data show that the largest matrix elements are of the operator $\mathcal{P}$; however, their net contribution to B_K^L is very small, since $\mathcal{P}^2 \sim 3\mathcal{P}^1$ (approximate VSA). Both T^2 and $\mathcal{V}^2$ are close to zero. The next largest contribution comes from $4\mathcal{T}^1$, which is partially canceled by $26\mathcal{S}^1+2\mathcal{S}^2$. The net result of these features in the data is that the contribution of mixing terms to B_K is in fact small (less than 10%).

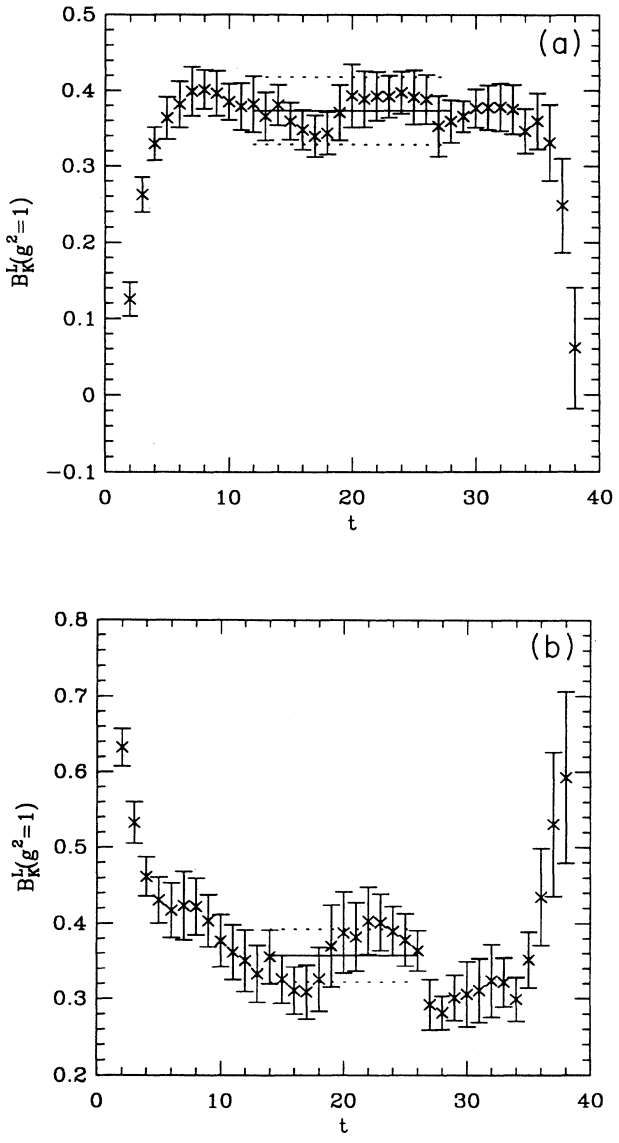

FIG. 1. (a) The ratio of correlators for the lattice parameter B_K^L ($g^2=1$, $\mu a=1.0$) at $\kappa=0.154$ and for momentum transfer $\mathbf{p}=(0,0,0)$. The data are obtained using operator γ_3 as the kaon source. (b) The same as in (a), but using operator A_4 as the kaon source.

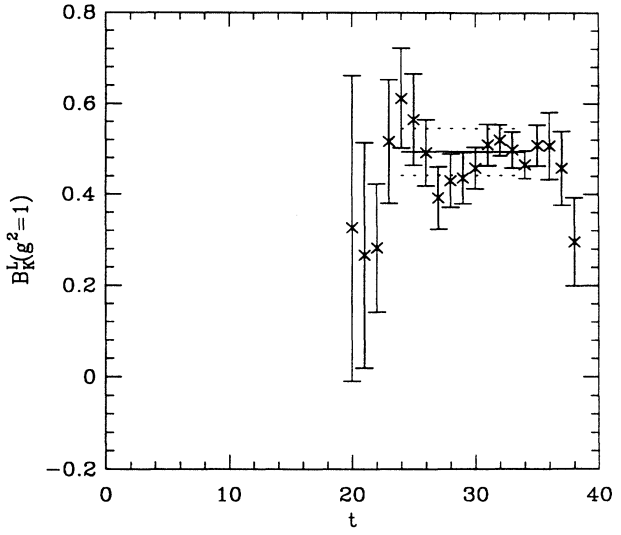

FIG. 2. The same as in Fig. 1(a), but for $\kappa=0.154$ and $\mathbf{p}=(0,0,1)$.

Given $B_K^L(\mathbf{p})$ we calculate B_K and the errors using Eq. (2.10) two ways: (1) for each jackknife sample we first perform the momentum subtraction and then the mean value and the error are obtained as the jackknife estimate over 35 samples, and (2) we construct the four quantities needed in Eq. (2.10) independently along with their errors, and obtain the final error estimate assuming that the individual estimates are uncorrelated. Our quoted results use the first method, but we note that both the methods yield consistent estimates.

We have calculated $B_K^L(\mathbf{p}=(0,0,0))$ three different ways: using Wuppertal-Wuppertal (*S-S*), Wuppertal-wall (*S-W*), and wall-wall (*W-W*) correlators. For example, our results, using $g^2=1.0$ and $\mu a=1.0$, are

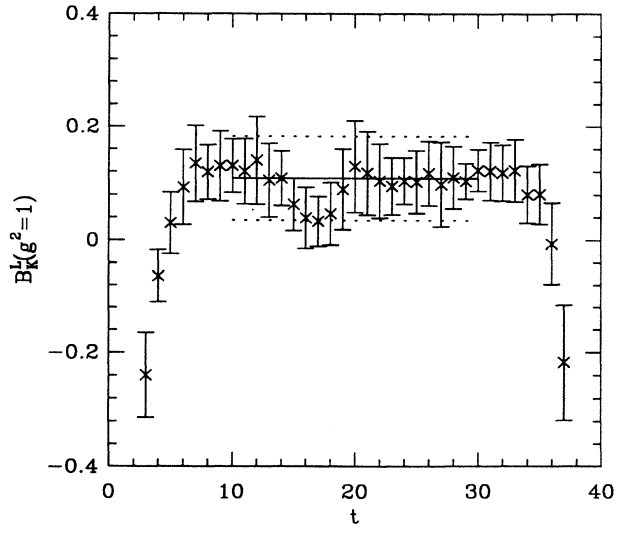

FIG. 3. The same as in Fig. 1(a), but for $\kappa=0.155$ and $\mathbf{p}=(0,0,0)$.

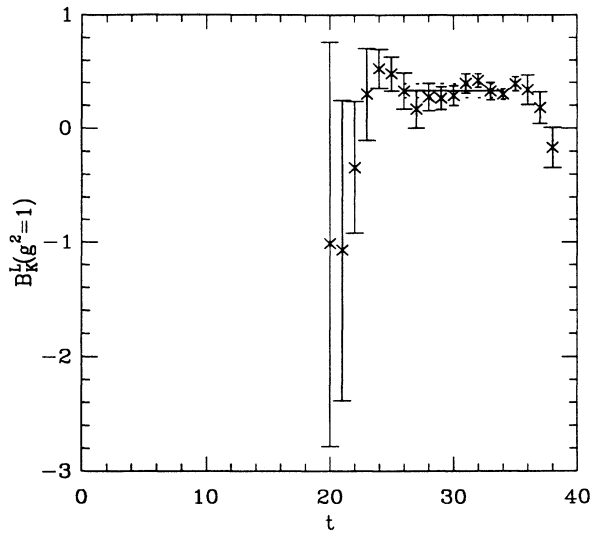

FIG. 4. The same as in Fig. 1(a), but for $\kappa=0.155$ and $\mathbf{p}=(0,0,1)$.

$$B_K^L(\kappa=0.154)=\begin{cases}0.38(7) & S\text{-}S,\\ 0.37(4) & S\text{-}W,\\ 0.37(4) & W\text{-}W,\end{cases} \tag{4.2}$$

$$B_K^L(\kappa=0.155)=\begin{cases}0.10(11) & S\text{-}S,\\ 0.11(7) & S\text{-}W,\\ 0.13(7) & W\text{-}W.\end{cases}$$

The consistency of the data suggests that the contamination in the S-S result from higher-momentum kaon states is at most a few percent. Correlated error analysis of data at $\mathbf{p}=(0,0,0)$ and $(0,0,1)$ using the jackknife process can only be done with the S-W correlators, so we shall henceforth quote results for $B_K^L(\mathbf{p})$ obtained from these.

In order to extract the continuum result for B_K we must choose the values of both g^2 and μa to use in Eq. (4.1). Lepage and Mackenzie have suggested [18] that perturbation theory is much better behaved if one uses the coupling constant in a continuum scheme such as the modified minimal subtraction scheme ($\overline{\text{MS}}$), instead of the bare lattice g^2. They also give a prescription for choosing the appropriate scale of the coupling constant. In general this scale will differ for the various operators that mix with $\mathcal{O}_+$ in Eq. (4.1). To simplify the calculation we take all the scales, and thus all the coupling constants, to be the same, i.e., all of $O(\pi/a)$. Then the Lepage-Mackenzie prescription amounts to a replacement of the bare lattice g^2 with an effective coupling $g^2_{\text{eff}}\approx 1.75g^2$ at $\beta=6.0$. To study the dependence on g^2_{eff}, we use four different values, $g^2_{\text{eff}}=0.0$, 1.0, 1.338, and 1.75. It is important to realize that only a two-loop calculation of the perturbative coefficients can test whether a given choice for g^2_{eff} is reasonable. Such calculations that have been done to date support the Lepage-Mackenzie prescription for choosing g^2_{eff} [18].

The choice of μa is of a different character than that of g^2. In physical matrix elements (e.g., that related to CP violation in K^0-$\bar{K}^0$ mixing) B_K always appears multiplied by a coefficient function, such that the combination is independent of μ. At leading order, the scale-independent combination is

$$\hat{B}_K=\alpha_s(\mu)^{-6/(33-2N_f)}B_K(\mu)\ , \tag{4.3}$$

where N_f is the number of active flavors. In fact, $\hat{B}_K$ does have some dependence on μ, coming from the following sources. First, since we are using only the leading order expression for $Z(\mu a)$, $\hat{B}_K$ does depend on μ at nonleading order: $d\ln\hat{B}_K/d\ln\mu\propto g^4(\mu)$. This is likely to be a small effect, and it can probably be pushed to next order given the fact that the two-loop anomalous dimension and one-loop matching coefficients are known. We say "probably" because it is possible that there are some residual subtleties with Wilson fermions associated with the mixing of $\mathcal{O}_+$ with opposite chirality operators. A related source of μ dependence occurs when μa differs greatly from unity: then higher-order terms, proportional to $[g^2\ln(\mu a)]^n$, which are not included in Eq. (4.1), become large. What is happening is that the leading logarithms, which have been summed into the coefficient function, are partially incorporated into the perturbative coefficients. Once again, one can probably take these into account knowing the anomalous dimension to two-loops, or finesse the problem by taking $\mu a\sim 1$. Finally, we are calculating the lattice result in the quenched approximation, for which the number of active flavors is zero, while we wish to match to the full theory with N_f active flavors. This introduces a small μ dependence.

Our emphasis in this paper is on improving methods for calculating B_K, and not on extracting final numbers for $\hat{B}_K$. Thus we choose to quote our results for a variety of values of μa so as to allow others some flexibility if they wish to use our numbers. We use $\mu a=1.0$, π, and 1.7π. We have a slight preference for $\mu a=\pi$, since then the continuum and lattice cutoffs are matched.

Table IV shows the sensitivity of the results to the choices of parameters, for both B_K^L and the momentum subtracted B_K. There is a significant variation of the results with g^2_{eff} and μa. For a fixed value of μa, the lattice results for both $B_K^L(\mathbf{p}=(0,0,0))$ and $B_K^L(\mathbf{p}=(0,0,1))$ increase as a function of g^2_{eff} due to the increased contribution of the mixing operators. For fixed g^2_{eff}, an increase in μa decreases the contribution of the diagonal operators [note that $B_K^L(\mathbf{p}=(0,0,0))$ at $\kappa=0.155$ is insensitive to changes in μa because the diagonal contribution happens to be almost zero there].

As for B_K after momentum subtraction, the estimate decreases by 10%–20%, at both values of quark mass, between $g^2_{\text{eff}}=1.0$ and $g^2_{\text{eff}}=1.75$, for fixed μa. It turns out that almost all the variation comes from the diagonal renormalization constants [for example, the ratio of $(1+(g^2/16\pi^2)Z_+)$ to Z_A^2 changes from 0.93 to 0.8], and not from operator mixing. As our present best estimates for B_K we quote the results at $g^2_{\text{eff}}=1.75$, and use $\mu a=\pi$:

TABLE IV. The lattice B parameter for the perturbatively improved operator $\hat{O}$ for zero and one unit of lattice momentum, and the B parameter after momentum subtraction. The data show the magnitude of the variation with the value of $g^2_{\rm eff}$ and μa used in the perturbative renormalization constants. The range of time slices used in the fits is specified in the header.

		$\kappa=0.154$			$\kappa=0.155$		
$g^2_{\rm eff}$	μa	$B_K^L(\mathbf{p}=0)$ 12–28	$B_K^L(\mathbf{p}=1)$ 24–34	B_K	$B_K^L(\mathbf{p}=0)$ 10–30	$B_K^L(\mathbf{p}=1)$ 26–34	B_K
0.00		0.298(44)	0.446(42)	0.83(21)	−0.023(63)	0.263(62)	0.77(19)
1.00	1.0	0.373(45)	0.494(52)	0.81(23)	0.109(74)	0.330(61)	0.71(20)
1.00	π	0.362(42)	0.476(50)	0.78(22)	0.110(71)	0.319(60)	0.69(22)
1.00	1.7π	0.356(42)	0.468(50)	0.76(22)	0.110(70)	0.315(59)	0.67(21)
1.338	1.0	0.405(44)	0.512(55)	0.79(24)	0.175(75)	0.359(69)	0.68(24)
1.338	π	0.388(42)	0.486(53)	0.75(22)	0.176(71)	0.344(62)	0.64(22)
1.338	1.7π	0.380(41)	0.475(51)	0.72(22)	0.176(69)	0.337(61)	0.62(22)
1.75	1.0	0.453(45)	0.536(58)	0.75(23)	0.268(70)	0.401(74)	0.64(25)
1.75	π	0.429(42)	0.497(53)	0.68(22)	0.268(63)	0.379(71)	0.57(23)
1.75	1.7π	0.417(41)	0.497(51)	0.64(21)	0.268(59)	0.369(69)	0.55(22)

$$B_K(\kappa=0.154)=0.68(22)\ ,$$
$$B_K(=0.155)=0.57(23)\ . \tag{4.4}$$

We now turn to the sources of systematic error in our results for B_K. We first address the question of p^4 terms in the chiral expansion. There are three terms at this order, $\delta_1 m^4$, $\delta_2 m^2 p\cdot p'$, and $\delta_3 p\cdot p' p\cdot p'$, the latter two containing a physical part as well as an artifact. There are also chiral logarithms [proportional to $m^4\ln(m)$ and possibly $m^2\ln(m)$], which we ignore. The momentum subtraction method removes $\delta_1 m^4$. So what we end up calculating is

$$\frac{E_K B_K(p)-m_K B_K(0)}{E_K-m_K}=\frac{(\gamma+\gamma_K)+\delta_2 m_K^2+\delta_3 m(m+E)}{8/3f_K^2}\ . \tag{4.5}$$

To disentangle δ_2 and δ_3 requires data at more values of momentum transfer. We can only roughly estimate the size of the $O(p^4)$ corrections by lumping all the corrections into a single term; i.e., we modify Eq. (4.5) to

$$\frac{E_K B_K(p)-m_K B_K(0)}{E_K-m_K}=\frac{(\gamma+\gamma_K)+\delta m(m+E)}{8/3f_K^2}\ . \tag{4.6}$$

Using our results at the two masses we extract $\delta\sim 0.02$. From this we find that the p^4 term is roughly [0.36,0.27] compared to [0.78,0.69] for the signal for B_K. These corrections are of similar size to those found using staggered fermions, i.e., 20%–30% at the physical kaon mass. Even though this comparison indicates that the $O(p^4)$ artifacts due to the chiral-symmetry-breaking term in Wilson fermions may be small, one needs to further develop a reliable way to extract the physical contribution.

The second source of error is the lattice artifact γ. To estimate this, we first extract the other artifacts, $\alpha+\beta m_K^2$, neglecting the $O(p^4)$ term. We find (using $g^2=1$, $\mu a=\pi$) that this combination is $[-10(6),-8(4)]\times 10^{-4}$, for $\kappa=[0.154,0.155]$. This is to be compared with our results for B_K, which can be represented as $(\gamma+\gamma_K)m_K^2=[19(5),10(3)]\times 10^{-4}$. Thus the artifacts are nearly as large as the signal. If we now use the estimate given in Sec. II, $\gamma/(\alpha+\beta M_K^2)\approx -0.3$, then we see that removing γ would reduce B_K by 15%–25%. We stress that this is only a crude estimate, but it does indicate that the error from this source is relatively small.

V. COMPARISON WITH PREVIOUS CALCULATIONS

The staggered fermion results for B_K [3] are statistically the most accurate and have the correct chiral behavior. At $\beta=6.0$, the kaon mass roughly matches for staggered $m_q=(0.02+0.03)$ and $\kappa=0.154$, and for staggered $m_q=(0.01+0.02)$ and $\kappa=0.155$ [19]. Thus we can compare the corresponding data for B_K. This is a particularly good comparison because the two calculations have been done using the same set of background gauge configurations. Using $g^2=0$ in the four-fermion renormalization constants, the staggered results are 0.76(1) and 0.72(2) to be compared with our numbers 0.83(21) and 0.77(19), respectively. A striking feature is that the errors with Wilson fermions are a factor of 10 or more larger. The data in Table IV indicate that the errors in individual $B_K^L(p)$ are larger by about a factor of 4, and the remaining factor comes from the momentum subtraction. The staggered results were obtained by making fits without including the full covariance matrix, and if we do the same for Wilson fermions then the errors in individual $B_K^L(p)$ are reduced by a factor of about 2. Thus, at the level of the signal in the correlators, the smeared sources work almost as well for Wilson fermions as for staggered fermions. It is the process of momentum subtraction that leads to a significant increase in the error.

The perturbative corrections for staggered fermions, though smaller than those for Wilson fermions, have not been included in the published results of B_K; including them would decrease B_K by $\approx(3g^2_{\rm eff})\%$ for the choice $\mu a=\pi$ [20]. It could be argued that one should actually compare corrected staggered numbers with our preferred results using $g^2_{\rm eff}=1.75$ and $\mu a=\pi$, i.e., 0.68(22) and 0.57(23), respectively. In this case Wilson fermion esti-

mates of B_K lie below the staggered values. (The variation with $g^2_{\rm eff}$ and μa is much larger for Wilson fermions.) To conclude, it is, at present, not clear whether the difference in B_K from the two formulations is significant, given the size of the errors in the Wilson results. Also, the differences in the $O(a)$ corrections for the two fermion formulations, e.g., the artifact γ, are not understood and have not been included in the comparison.

We can also make a direct comparison with results obtained by Bernard and Soni using Wilson fermions [2]. They have calculated $B_K^L(\mathbf{p}=0)$ using the perturbatively improved operator on a subset of the same lattices (they used only 19 lattices as they skipped every other one in each of the two streams), and at the same two values of κ. Their method of extraction of B_K^L is described in Ref. [2], and is different than the method we have used. Using $g^2_{\rm eff}=1.338$ and $\mu a=1.7\pi$ their results are $B_K^L(\mathbf{p}=0)=0.36(22)$ and $0.24(45)$ at $\kappa=0.154$ and 0.155, respectively [15], to be compared with $B_K^L(\mathbf{p}=0)=0.38(5)$ and $0.11(7)$ obtained by us. Even after allowing for a factor of $\sim\sqrt{2}$ due to statistics, it is clear on the basis of this comparison that our use of smeared sources has reduced the errors considerably.

Though our results for B_K^L are more accurate compared to those obtained by other groups using Wilson fermions, our final results for B_K have larger errors [cf. Eqs. (1.2) and (1.3)]. The gain due to the use of smeared sources is compensated for by the increase in error due to momentum subtraction. The advantage of using momentum subtraction is that it unambiguously removes lattice artifacts α and β. Also, numerical errors in $B_K^L(\mathbf{p}=1)$, as well as the contribution of quartic terms in the chiral expansion, should decrease when using a larger lattice due to the decrease in the value of lattice momenta.

One further qualitative comparison that we can make is for the B parameters (without perturbative improvements but after momentum subtraction) of the individual space-time and one-loop and/or two-loop components of the four-fermion vector and axial-vector operators, with the corresponding results obtained using staggered fermions [3]. Such a comparison is possible because, as discussed above, the effects of operator mixing are small. This comparison provides information on the reliability of the momentum subtraction procedure for Wilson fermions. Furthermore, as explained in Ref. [21], the chiral behavior of $B_{\mathcal{V}}$ and $B_{\mathcal{A}}$ is known; both are expected to increase in magnitude with decreasing quark mass due to chiral logarithms and finite volume dependence, and can therefore provide a sensitive test at small quark masses. The results of our comparison are shown in Table V. Though the errors in the results with Wilson fermions are much larger, it is reassuring to see that the central values are in good agreement. In fact, the agreement is far more impressive than the errors would naively lead us to believe. We need to perform calculations at more values of κ and β to confirm this favorable behavior.

VI. RESULTS WITH TWO FLAVORS OF DYNAMICAL FERMIONS

We have also estimated B_K, using the same methodology as above, on 16^4 lattice configurations generated with two flavors of dynamical Wilson quarks. The details of these lattices are given in Ref. [22]. The kaon mass at $\beta=5.5$, $\kappa=0.159$ and 0.160 is roughly $M_K=860$ and 650 MeV, respectively; and at $\beta=5.6$, $\kappa=0.156$ and 0.157 it is about 1050 and 820 MeV, respectively. This calculation of B_K has been done only with kaons created with a γ_5 operator. We find that a time interval of 16 is large enough to give a stable plateau over about six central time slices for both $\mathbf{p}=(0,0,0)$ and $(0,0,1)$ correlators, as illustrated in Figs. 5 and 6. The behavior of individual $B_{\mathcal{O}}$ terms is very similar to the quenched numbers shown in Tables II(a)–III(b).

Before presenting the final results, we first discuss a technical drawback of this calculation. On these lattices only Wuppertal source correlators are available, so with our method some contamination from higher-momentum kaon states is present in the data. For momentum

TABLE V. A comparison of individual B parameters, for space-time and one-loop and/or two-loop components of the vector and axial-vector four-fermion operators, between Wilson and staggered fermions at matching values of the kaon mass. The kaon energy at $\mathbf{p}=(0,0,0)$ and $\mathbf{p}=(0,0,1)$ measured from the two-point correlators is also given. All results are quoted for $g^2_{\rm eff}=0$.

	Wilson $\kappa=0.154$	Staggered $m_q=0.02+0.03$	Wilson $\kappa=0.155$	Staggered $m_q=0.01+0.02$
M_K	0.370(6)	0.374(3)	0.297(11)	0.296(2)
E_K	0.511(12)		0.466(22)	
$\mathcal{V}_s^1$	−0.57(33)	−0.48(2)	−0.71(53)	−0.79(4)
$\mathcal{V}_s^2$	−0.11(8)	−0.036(4)	−0.13(11)	−0.10(1)
$\mathcal{V}_t^1$	−0.10(7)	−0.056(3)	−0.12(15)	−0.13(1)
$\mathcal{V}_t^2$	0.01(2)	−0.009(1)	−0.02(4)	−0.024(2)
$\mathcal{A}_s^1$	0.28(18)	0.15(1)	0.41(42)	0.36(2)
$\mathcal{A}_s^2$	0.27(16)	0.063(5)	0.29(32)	0.13(1)
$\mathcal{A}_t^1$	0.28(12)	0.33(1)	0.40(20)	0.42(1)
$\mathcal{A}_t^2$	0.79(26)	0.81(1)	0.82(40)	0.85(2)
$B_{\mathcal{A}}$	1.62(42)	1.35(3)	1.92(89)	1.76(5)
$B_{\mathcal{V}}$	−0.78(40)	−0.58(2)	−0.98(71)	−1.04(5)
B_K	0.83(21)	0.76(1)	0.77(19)	0.72(2)

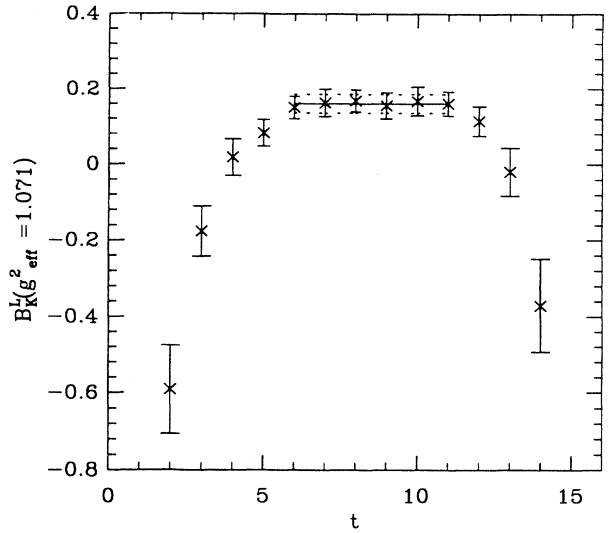

FIG. 5. The ratio of correlators for the lattice parameter B_K^L ($g^2_{\rm eff}=1.071$, $\mu a=1$) measured on 16^4 lattices generated with two degenerate flavors of dynamical Wilson fermions. The lattice parameters are $\beta=5.6$, $\kappa=0.157$, and momentum transfer $\mathbf{p}=(0,0,0)$, and we use $\bar{s}\gamma_5 d$ as the kaon source.

transfer $\mathbf{p}=(0,0,0)$, the largest contamination comes from the propagation of $\mathbf{p}=(0,0,1)$ kaons across the lattice. [The contamination in the $\mathbf{p}=(0,0,0)\rightarrow(0,0,1)$ data comes from the presence of $\mathbf{p}=(0,0,1)\rightarrow(0,0,2)$ terms.] This contribution is suppressed by two factors: the exponential suppression due to the extra energy of the $\mathbf{p}=(0,0,1)$ state, and the square of the ratio of amplitudes for creating a $\mathbf{p}=(0,0,1)$ kaon versus a $\mathbf{p}=(0,0,0)$ kaon by the Wuppertal source. These factors increase as the kaon mass decreases. They are similar on our four sets of lattices. At $\beta=5.6$ and $\kappa=0.157$, our estimates are ≈ 10 and $(1.5)^2$. There is also an enhancement factor because the matrix element between higher-momentum

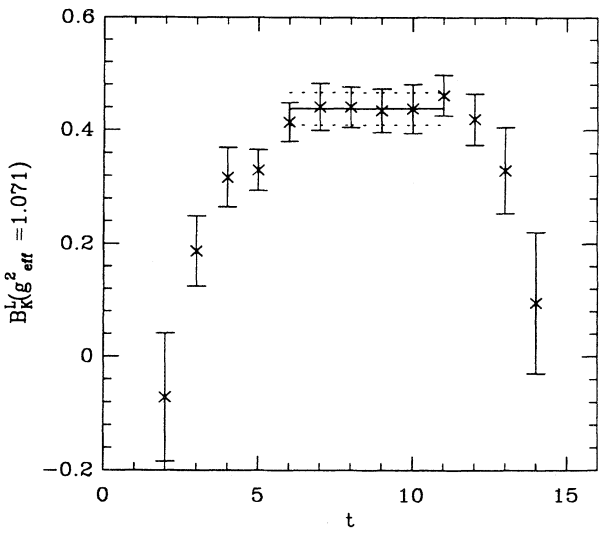

FIG. 6. The same as in Fig. 5 but for $\mathbf{p}=(0,0,1)$.

kaon states is larger. We estimate this factor using the VSA to be $(E(p=1)/M_K)^2\approx(1.5)^2$. These three factors combine to increase the result for B_K by roughly 10%. We note that in the case of the quenched lattices, having 40 time slices reduced this contamination to the level of a few percent. This is evident when comparing the S-S and the S-W or the W-W results in Tables II(a)–III(b).

We again calculate B_K^L for three values of the effective coupling: 0.0, g^2, and $1.75g^2$. The lattice scale on individual lattices (without extrapolation to the chiral limit) is not well defined, and we simply set $\mu a=1$. The results are shown in Table VI. As explained above, the results for B_K are likely to be $\sim 10\%$ larger due to contamination from higher-momentum kaon states. In addition, B_K has to be extrapolated to the physical kaon mass. Thus, the only conclusion we can draw is that the quenched and dynamical results are in qualitative agreement for quarks masses in the range $m_s<m_q<3m_s$.

VII. B PARAMETER FOR THE LEFT-RIGHT ELECTROMAGNETIC PENGUIN OPERATORS

There are two additional four-fermion operators that we analyze using the data in Tables II(a)–III(b). These are the $\Delta I=\frac{3}{2}$ part of the left-right electromagnetic penguin operators $\mathcal{O}_7$ and $\mathcal{O}_8$. They alone contribute to the imaginary part of the $I=2$ amplitude and therefore give the dominant electromagnetic contribution to ϵ'/ϵ. A knowledge of their B parameters is phenomenologically important as discussed in Ref. [23]. Taking just the $\Delta I=\frac{3}{2}$ part of the operators simplifies the numerical calculation as the "eye" contractions cancel in the flavor SU(2) limit.

In principle one would like to calculate the matrix elements of the penguin operators

$$\mathcal{O}_7=(\bar{s}_a\gamma_\mu Ld_a)[(\bar{u}_b\gamma_\mu Ru_b)-\tfrac{1}{2}(\bar{d}_b\gamma_\mu Rd_b)-\tfrac{1}{2}(\bar{s}_b\gamma_\mu Rs_b)]\,, \tag{7.1}$$

$$\mathcal{O}_8=(\bar{s}_a\gamma_\mu Ld_b)[(\bar{u}_b\gamma_\mu Ru_a)-\tfrac{1}{2}(\bar{d}_b\gamma_\mu Rd_a)-\tfrac{1}{2}(\bar{s}_b\gamma_\mu Rs_a)]\,, \tag{7.2}$$

between a K^+ and a π^+. Instead, we calculate the $\Delta I=\frac{3}{2}$ part given by the operators

$$\mathcal{O}_7^{3/2}=(\bar{s}_a\gamma_\mu Ld_a)[(\bar{u}_b\gamma_\mu Ru_b)-(\bar{d}_b\gamma_\mu Rd_b)]+(\bar{s}_a\gamma_\mu Lu_a)(\bar{u}_b\gamma_\mu Rd_b)\,, \tag{7.3}$$

$$\mathcal{O}_8^{3/2}=(\bar{s}_a\gamma_\mu Ld_b)[(\bar{u}_b\gamma_\mu Ru_a)-(\bar{d}_b\gamma_\mu Rd_a)]+(\bar{s}_a\gamma_\mu Lu_b)(\bar{u}_b\gamma_\mu Rd_a)\,. \tag{7.4}$$

Note that the overall normalization is unimportant as it cancels in the B parameters. The one loop perturbatively corrected versions of these operators have been calculated in Refs. [11,12], and are linear combinations of the operators labeled $\mathcal{O}_1$ and $\mathcal{O}_2$ therein. The matrix elements of these corrected operators between a K^+ and a π^+ are, in the flavor SU(2) limit,

TABLE VI. The same as in Table IV, but for lattices generated with two flavors of dynamical Wilson quarks. The upper and lower halves of the table correspond to $\beta=5.5$ and $\beta=5.6$, respectively. These numbers are obtained with $\mu a=1.0$.

		$B_K^L(0)$	$B_K^L(1)$	M_K	$E(1)$	B_K
$\kappa=0.159$	$g^2_{\rm eff}=0.000$	0.327(88)	0.507(96)			0.98(43)
	$g^2_{\rm eff}=1.091$	0.389(74)	0.537(80)	0.477(13)	0.660(16)	0.92(36)
	$g^2_{\rm eff}=1.909$	0.401(56)	0.505(58)			0.78(27)
$\kappa=0.160$	$g^2_{\rm eff}=0.000$	−0.593(88)	−0.052(51)			0.93(24)
	$g^2_{\rm eff}=1.091$	−0.415(76)	0.051(44)	0.362(7)	0.562(22)	0.89(21)
	$g^2_{\rm eff}=1.909$	−0.217(57)	0.132(34)			0.76(17)
$\kappa=0.156$	$g^2_{\rm eff}=0.000$	0.497(33)	0.685(39)			1.23(20)
	$g^2_{\rm eff}=1.071$	0.534(31)	0.693(36)	0.456(5)	0.613(10)	1.15(19)
	$g^2_{\rm eff}=1.875$	0.512(26)	0.629(30)			0.97(16)
$\kappa=0.157$	$g^2_{\rm eff}=0.000$	0.154(25)	0.436(29)			1.14(19)
	$g^2_{\rm eff}=1.071$	0.161(25)	0.438(29)	0.358(7)	0.501(16)	1.13(19)
	$g^2_{\rm eff}=1.875$	0.234(21)	0.439(24)			0.95(16)

$$\mathcal{M}_7(\mathbf{p})=\left[1+\frac{g^2}{16\pi^2}Z_1(r,a\mu)\right][2\mathcal{P}^1-2\mathcal{S}^1+\mathcal{V}^2-\mathcal{A}^2]+\frac{g^2}{16\pi^2}\frac{(Z_2-Z_1)}{3}[2\mathcal{P}^2-2\mathcal{S}^2+\mathcal{V}^1-\mathcal{A}^1]$$
$$+\frac{g^2}{16\pi^2}\frac{r^2Z^*(r)}{12}[4\mathcal{P}^1-12\mathcal{P}^2+16\mathcal{S}^1-16\mathcal{S}^2-7\mathcal{V}^1-11\mathcal{V}^2-9\mathcal{A}^1-5\mathcal{A}^2-6\mathcal{T}^1+2\mathcal{T}^2] \tag{7.5}$$

and

$$\mathcal{M}_8(\mathbf{p})=\left[1+\frac{g^2}{16\pi^2}Z_2(r,a\mu)\right][2\mathcal{P}^2-2\mathcal{S}^2+\mathcal{V}^1-\mathcal{A}^1]$$
$$+\frac{g^2}{16\pi^2}\frac{r^2Z^*(r)}{12}[18\mathcal{P}^1-38\mathcal{P}^2+14\mathcal{S}^1-26\mathcal{S}^2-5\mathcal{V}^1-\mathcal{V}^2+\mathcal{A}^1-3\mathcal{A}^2-16\mathcal{T}^1]\,, \tag{7.6}$$

where, if necessary, we have made a spin Fierz transformation to recast all the terms as two-spinor loops. The corresponding VSA contractions are

$$\mathcal{M}_7^{\rm VSA}(\mathbf{p})=[\tfrac{2}{3}Z_P^2\mathcal{P}^2-Z_A^2\mathcal{A}^2] \tag{7.7}$$

and

$$\mathcal{M}_8^{\rm VSA}(\mathbf{p})=[2Z_P^2\mathcal{P}^2-\tfrac{1}{3}Z_A^2\mathcal{A}^2]\,. \tag{7.8}$$

The B parameters are the ratios of, for example, the matrix element of O_7 to its VSA. We evaluate these in the SU(3) limit, i.e., degenerate u, d, and s quarks. The one-loop values of the renormalization constants for these LR operators are also given in Table I. Note that in the DRED scheme the operator $\mathcal{O}_8^{3/2}$ does not mix with the scheme-dependent operator $\overline{\mathcal{O}}$ of Ref. [12]. It is for this reason that we choose this scheme, although our analysis shows that the results are only weakly scheme dependent.

In the chiral limit these matrix elements are expected to behave as $c+dm_\pi^2+\cdots$. There are $O(a)$ corrections in the coefficients c and d due to the lattice discretization. At present the only way to reduce these is to use an improved action and/or work at weaker coupling. In this study we do not have any control over these corrections and we simply give the lattice results for the Wilson action.

The quality of the signal is shown in Figs. 7 and 8. In the analysis of these LR operators we find that using the full covariance matrix produced estimates that are about 1σ lower than the fit values shown unless we significantly decrease the range of the fit. The error estimates with and without using the full covariance matrix in the fits are essentially the same. This indicates that the data at

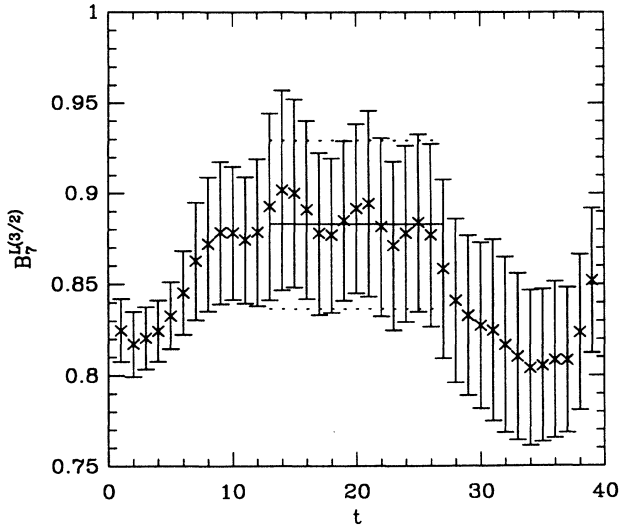

FIG. 7. B parameter for the LR electromagnetic penguin operator $\mathcal{O}_7^{3/2}$. The data are obtained using $g^2_{\rm eff}=1.75$ and $\mu a=\pi$.

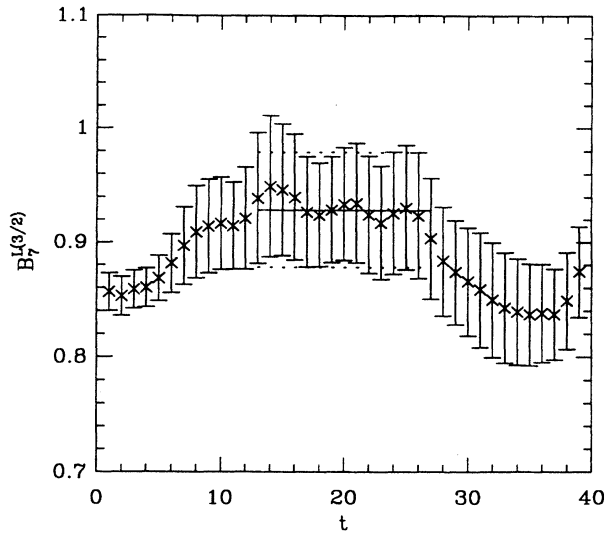

FIG. 8. B parameter for the LR electromagnetic penguin operator $\mathcal{O}_8^{3/2}$. The data are obtained using $g^2_{\rm eff}=1.75$ and $\mu a=\pi$.

different time slices are highly correlated and larger statistics is needed to reliably include the correlations. We choose to use the full range of the plateau in the fit and quote results obtained without including the correlations.

As in the case of the LL operator, in order to quote a value for the B parameters we have to specify the value of $g^2_{\rm eff}$ and μa used in the perturbatively improved operators. In Table VII we quote results for a number of choices in order to give an estimate of the sensitivity of the results to variation in these parameters. The data show that this could be a 10% effect, so it is important to make a good choice of $g^2_{\rm eff}$.

The data also show a small increase in the B parameters as the quark mass is decreased. Linearly extrapolating the $g^2_{\rm eff}=1.75$, $\mu a=\pi$ results to the physical kaon mass, our best estimates are

$$B_7^{3/2}=0.89(4)\ ,\qquad B_8^{3/2}=0.93(5)\ . \tag{7.9}$$

These values are slightly smaller than the numbers used by Lusignoli *et al.* [23] in their analysis of ϵ'/ϵ; they used $B_7^{3/2}=B_8^{3/2}=1.0\pm0.1$. To make a complete determination of ϵ'/ϵ we need to calculate many other matrix elements, for example of the strong penguin operators $\mathcal{O}_5$ and $\mathcal{O}_6$, for which the lattice technology is still unreliable. For this reason we do not consider it opportune to repeat the phenomenological analysis.

We can make a direct comparison of lattice results for $\mathcal{O}_7^{3/2}$ with those obtained by Bernard and Soni on the subset of lattices described in the analysis of B_K. Their result, obtained using $g^2_{\rm eff}=1.338$ and $\mu a=1.7\pi$ in the DR($\overline{\rm EZ}$) scheme, is 0.965(41) at $\kappa=0.155$, to be compared with 0.971(50) obtained by us. This comparison suggests that for the matrix elements of LR operators, our method of sandwiching the operator between smeared sources is no better than using propagators from a single source point. On the other hand, the fact that smeared sources yield a plateau over a large range of time slices gives reassurance that one potential source of systematic error is under control.

VIII. CONCLUSIONS

We show that the calculation of the kaon B parameters with Wilson fermions is significantly improved by the use of nonlocal quark sources. By using a combination of Wuppertal and wall source correctors, we demonstrate that the on-shell matrix elements can be calculated at nonzero momenta.

By combining results at $\mathbf{p}=(0,0,0)$ and $(0,0,1)$, we carry out a nonperturbative subtraction of the lattice artifacts in the calculation of B_K. Even though we cannot take into account the artifact γ, our results are in good agreement with those obtained with staggered fermions. On the basis of this exploratory study we feel confident that the momentum subtraction procedure indeed works. To make further improvements and reduce the $O(a)$ artifacts one needs to repeat the calculations with an improved lattice action and on a larger physical lattice with smaller $\mathbf{p}_{\rm min}$.

We find a clean plateau in the data for the B parameters of the LR electromagnetic penguin operators. The

TABLE VII. The B parameter for the LR electromagnetic penguin operators on the quenched lattices. The fit range is $t=13$–27 in all cases. The results are shown for a number of values of $g^2_{\rm eff}$ and μa used in the perturbative renormalization constants.

		$\kappa=0.154$		$\kappa=0.155$	
$g^2_{\rm eff}$	μa	$\mathcal{O}_7^{3/2}$	$\mathcal{O}_8^{3/2}$	$\mathcal{O}_7^{3/2}$	$\mathcal{O}_8^{3/2}$
0.00		0.902(24)	0.947(30)	0.908(44)	0.963(50)
1.00	1.0	0.871(24)	0.918(29)	0.878(44)	0.935(50)
1.00	π	0.918(29)	0.945(30)	0.911(46)	0.962(52)
1.00	1.7π	0.901(25)	0.953(30)	0.921(46)	0.969(52)
1.338	1.0	0.832(23)	0.877(23)	0.830(43)	0.894(48)
1.338	π	0.891(25)	0.934(30)	0.902(46)	0.951(51)
1.338	1.7π	0.908(25)	0.950(30)	0.921(47)	0.966(52)
1.75	1.0	0.747(21)	0.785(26)	0.753(40)	0.802(45)
1.75	π	0.869(25)	0.911(30)	0.883(46)	0.928(51)
1.75	1.7π	0.901(26)	0.941(31)	0.916(48)	0.958(52)

results show that the VSA works much better for these operators. All the B parameters vary significantly with the choice of $g^2_{\rm eff}$ used in the perturbative renormalization coefficients. Our final estimates are given using the value advocated by Lepage and Mackenzie in Ref. [18], i.e., $g^2_{\rm eff}=1.75$.

The method of using the combination of Wuppertal and wall correctors can be extended to study other three-point correlation functions, in particular structure functions and form factors. This work is in progress.

ACKNOWLEDGMENTS

We thank C. Bernard and G. Martinelli for providing unpublished data and for discussions. The $16^3\times 40$ lattices were generated at NERSC at Livermore using a DOE allocation. The calculation of quark propagators and the analysis have been done at the Pittsburgh Supercomputing Center, San Diego Supercomputer Center, NERSC, and Los Alamos National Laboratory. We are very grateful to Jeff Mandula, Norm Morse, Ralph Roskies, Charlie Slocomb, and Andy White for their support of this project. This research was supported in part by the National Science Foundation under Grant No. PHY89-04035. R.G., G.W.K., A.P., and S.R.S. thank the Institute for Theoretical Physics, Santa Barbara for hospitality during part of this work. A.P. also thanks Los Alamos National Laboratory for hospitality during the course of this work. G.W.K. was supported in part by DOE Outstanding Junior Investigator and NSF Presidential Young Investigator programs. S.R.S. was supported in part by DOE Contract No. DE-AC05-84ER40150 and by the Alfred P. Sloan Foundation.

[1] M. B. Gavela *et al.*, Nucl. Phys. **B306**, 677 (1988).
[2] C. Bernard and A. Soni, in *Lattice '89,* Proceedings of the International Symposium on Lattice Field Theory, Capri, Italy, 1989, edited by N. Cabibbo *et al.* [Nucl. Phys. B (Proc. Suppl.) **17**, 495 (1990)].
[3] G. Kilcup, S. Sharpe, R. Gupta, and A. Patel, Phys. Rev. Lett. **64**, 25 (1990).
[4] G. Martinelli, in *Lattice '89* [2], p. 266.
[5] G. Martinelli, C. T. Sachrajda, G. Salina, and A. Vladikas, Nucl. Phys. **B378**, 591 (1992).
[6] S. Güsken *et al.*, Phys. Lett. B **227**, 266 (1989); S. Güsken, in *Lattice '89* [2], p. 365.
[7] D. Daniel, R. Gupta, G. Kilcup, A. Patel, and S. Sharpe, Phys. Rev. D **46**, 3130 (1992).
[8] C. Bernard, T. Draper, G. Hockney, and A. Soni, in *Field Theory on the Lattice,* Proceedings of the International Symposium on Lattice Field Theory, Seillac, France, 1987, edited by A. Billoire *et al.* [Nucl. Phys. B (Proc. Suppl.) **4**, 483 (1988)].
[9] E. Franco, L. Maiani, G. Martinelli, and E. Morelli, Nucl. Phys. **B317**, 63 (1989).
[10] S. Sharpe, R. Gupta, G. Guralnik, G. Kilcup, and A. Patel, Phys. Lett. B **192**, 149 (1987).
[11] G. Martinelli, Phys. Lett. **141B**, 395 (1984).
[12] C. Bernard, T. Draper, and A. Soni, Phys. Rev. D **36**, 3224 (1987).
[13] G. Altarelli, G. Curci, G. Martinelli, and S. Petrarca, Nucl. Phys. **B187**, 461 (1981).
[14] A. Buras and P. Weisz, Nucl. Phys. **B333**, 66 (1990).
[15] C. Bernard and A. Soni (private communication).
[16] C. Bernard and A. Soni, in *Lattice '88,* Proceedings of the International Symposium on Lattice Field Theory, Batavia, Illinois, 1988, edited by A. S. Kronfeld and P. B. Mackenzie [Nucl. Phys. B (Proc. Suppl.) **9**, 155 (1989)].
[17] S. Sharpe, in *Lattice '89* [2], p. 146.
[18] G. P. Lepage and P. B. Mackenzie, in *Lattice '90,* Proceedings of the International Symposium on Lattice Field Theory, Tallahassee, Florida, 1990, edited by U. M. Heller *et al.* [Nucl. Phys. B (Proc. Suppl.) **20**, 173 (1991)]; Fermilab Report No. FERMILAB-PUB-19/355-T (9/92) (unpublished).
[19] R. Gupta, G. Guralnik, G. W. Kilcup, and S. R. Sharpe, Phys. Rev. D **43**, 2003 (1991).
[20] S. Sharpe, in *Standard Model, Hadron Phenomenology and Weak Decays on the Lattice,* edited by G. Martinelli (World Scientific, Singapore, 1993).
[21] S. Sharpe, Phys. Rev. D **46**, 3146 (1992).
[22] R. Gupta, C. Baillie, R. Brickner, G. Kilcup, A. Patel, and S. R. Sharpe, Phys. Rev. D **44**, 3272 (1991).
[23] M. Lusignoli, L. Maiani, G. Martinelli, and L. Reina, Nucl. Phys. **B369**, 139 (1992).